

## A Camouflage Device without Metamaterials

Fei Sun<sup>1</sup>, Yijie Zhang<sup>2</sup>, Julian Evans<sup>2</sup>, and Sailing He<sup>2, \*</sup>

**Abstract**—We propose a camouflage device that can greatly reduce scattering in the microwave frequency using only uniform copper plates with no internal structuring (no metamaterials). The camouflage device is designed by optical surface transformation (OST), which is derived from transformation optics but much simpler than transformation optics. The key of our design is to choose suitable arrangement and lengths of these copper plates that satisfy Fabry-Perot condition. The proposed camouflage device can work when the detecting wave comes from a wide-angle range (not only works for some discrete angles). The proposed method will give a new and simple way to design and realize camouflage device.

### 1. INTRODUCTION

With the development of transformation optics [1–3] and metamaterials [4–6], it is no longer a science fiction to achieve the idea of invisibility and camouflage. Experimental demonstrations across many spectral regimes [4–10] and types of field [11–14] have been reported. However, the enthusiasm for a practical full cloak has diminished due to the stringent requirements and challenging fabrication of metamaterials. Carpet-cloaks [15–17] can readily avoid the singularities but can only hide an object attached to a surface. Full-space invisibility cloaks guide waves around a concealed region creating two optically isolated spaces. From the perspective of transformation optics, a point-extended coordinate transformation can be utilized to design such optical isolation cloaks (OICs) [1, 3], which requires a singularity at the inner boundary of the cloak. Although the singularity can be removed by eikonal approximation, the performance of the reduced cloak is substantially reduced [4]. Landy et al. reported a full cloak that avoids singularities or approximations but only works for one particular detection angle (unidirectional cloak) using traditional transformation optics [6]. In this study, we use optical surface transformation (OST) to design a camouflage device that can greatly reduce the scatterings for a wide-continuous-angle detection (e.g., from +60 degree to –60 degree) and only requires one homogeneous anisotropic material. We also designed uniform metallic plates to realize the camouflage device in the microwave frequency without any reductions. Numerical simulations show very strong scattering suppression effect for both beam illumination and point sources.

### 2. THEORETICAL METHOD

OST is a new theoretical design method derived from transformation optics [18, 19] as a surface-to-surface correspondence method. Two surfaces linked by optic-null medium (ONM) are equivalent surfaces in OST [18]. OST is broadly applicable in the design of lenses [18, 20], electromagnetic open resonators [21], overlapped illusions [22], waveguide bends [23], scattering cover-up cloaks [24],

---

*Received 8 August 2019, Accepted 17 September 2019, Scheduled 25 September 2019*

\* Corresponding author: Sailing He (sailing@kth.se). Fei Sun and Yijie Zhang contributed equally to this work.

<sup>1</sup> Key Lab of Advanced Transducers and Intelligent Control System, Ministry of Education and Shanxi Province, College of Physics and Optoelectronics, Taiyuan University of Technology, Taiyuan 030024, China. <sup>2</sup> State Key Laboratory of Modern Optical Instrumentations, Centre for Optical and Electromagnetic Research, JORCEP, Zhejiang University, Hangzhou 310058, China.

subwavelength focusing [25], etc. ONM has extremely large permittivity and permeability along its main axis, and close to zero in orthogonal directions. The ONM serves as a perfect endoscope, which can project the electromagnetic field distribution from one surface identically onto another along its main axis. The ONM with its main axis along the  $x$  direction in Cartesian coordinate system can be expressed as:

$$\varepsilon = \mu = \text{diag} \left( \frac{1}{\Delta}, \Delta, \Delta \right), \quad \Delta \rightarrow 0. \quad (1)$$

The building block of our camouflage device is a shifter designed using OST. As shown in Fig. 1(a), the surfaces  $S_1$  and  $S_2$  with the same area are linked by an ONM of main axis along  $+45$  degree (the direction of main axis is indicated by the green arrow). The length of the shifter is  $d$  in the  $x$  direction. The shifted distance between  $S_1$  and  $S_2$  along the  $y$  direction is  $d$ . Numerical simulation shows that both phase and amplitude distributions on  $S_1$  are projected onto  $S_2$  through the ONM (see Fig. 1(b)). The designed shifter can also work for other incident angles (see Figs. 1(c)–(e)). Unlike electromagnetic shifters designed by transformation optics [26], the shifter designed by OST does not need any coordinate transformation or mathematical calculation to determine the material parameters of the device. All we need to do is to fix the relative position of input surface  $S_1$  and output surface  $S_2$ , and find the proper projecting direction to align the main axis of the ONM. With different length the shifter designed by transformation optics needs new material design. However, for electromagnetic wave shifter designed by OST, it only needs one homogeneous medium (ONM), no matter how other parameters change. Even if the geometrical size or shifted length changes, shifter designed by OST can

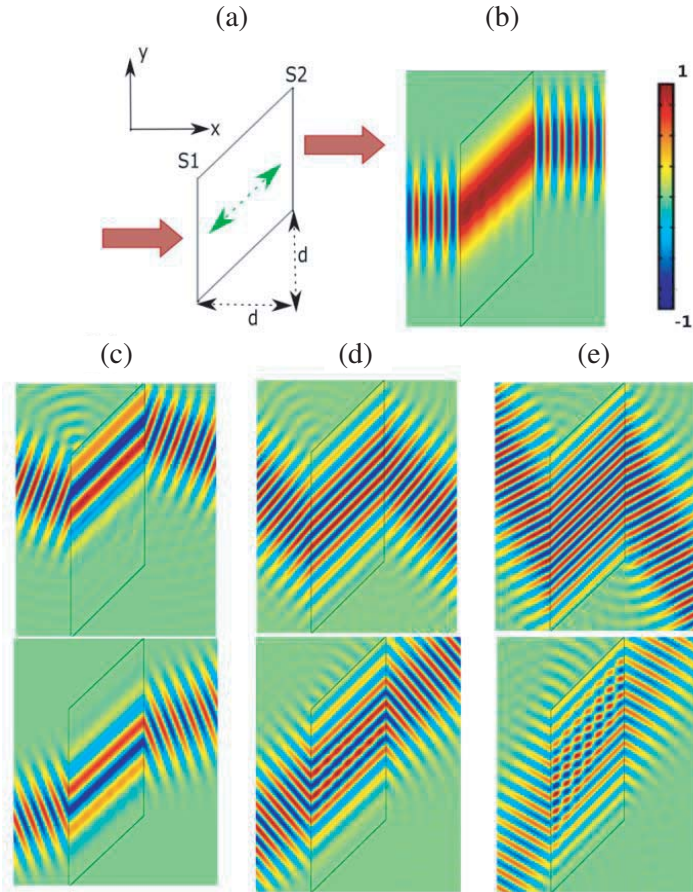


**Figure 1.** (a) Shifter schematic. (b)–(e) 2D numerical simulations for the designed shifter when the incident angles of the Gaussian beams are 0,  $\pm 20$ ,  $\pm 40$ , and  $\pm 60$  degrees. We plot snapshots of the normalized magnetic field's  $z$  component distribution for the TM wave case.

still be realized by the ONM (but with different main axis' direction). Later, we will show how to use metallic plates to realize ONM, which means that all kinds of shifters designed by OST can be realized by metallic plates.

Placing four electromagnetic shifters around a square of size  $\sqrt{2}d$  creates a region that no detecting wave can reach and achieves a concealed region (see Fig. 2(a)). From the perspective of OST, surfaces  $S_I$  and  $S_{II}$  (colored green) are equivalent surfaces: the electromagnetic wave incident onto  $S_{II}$  will be smoothly redirected around the concealed region and transmitted to  $S_I$  without being distorted. Similarly, surfaces  $S_{III}$  and  $S_{IV}$  (colored blue) are also equivalent surfaces, which can be treated as the mirror symmetry of  $S_{II}$  and  $S_I$  on  $x$  axis, respectively. The materials in regions I–IV are all ONM whose main axis is indicated by the red arrows (+45 degree for the regions II and IV;  $-45$  degree for the regions I and III). The regions II and III are the designed electromagnetic shifter. The regions I and IV are the mirror image of the designed shifter. The performance of designed camouflage device is verified by numerical simulations in Figs. 2(b)–(e), which shows this camouflage device can work effectively when the incident angle of the detecting beam illumination changes. In Figs. 2(b)–(e), we set a PEC boundary condition as the boundary of the concealed region in the central square. Some small scattering in Figs. 2(b)–(e) is mainly due to the finite height (along  $y$  direction) of our device. The effective working surfaces of our device are the front and back planes in Fig. 2(a). If the height of our

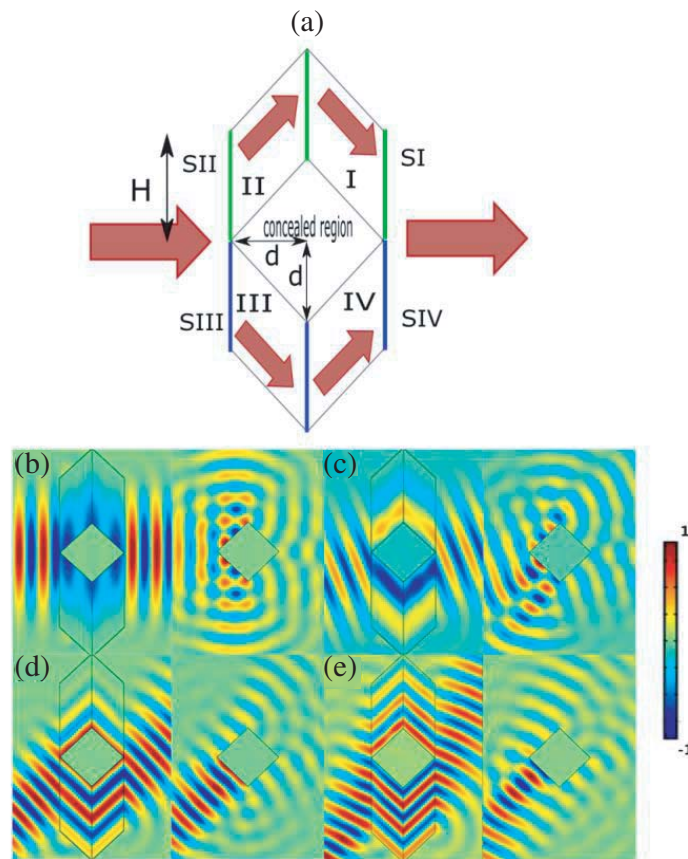


**Figure 2.** (a) The schematic diagram to design a camouflage device with four electromagnetic shifters. (b)–(e) 2D numerical simulations for the snapshots of the distributions for the normalized magnetic field's  $z$  component: the incident detecting waves are Gaussian beams with the same waist radius  $w_0 = 2\lambda_0$  when the incident angle changes from 0 degree to 60 degree by a 20-degree increments onto a PEC square wrapped by our camouflage device (Left) or onto only a PEC square without camouflage device (Right). The geometrical size of our camouflage device is size of each shifter in the OIC is  $d = \lambda_0 4/3$  and  $H = \lambda_0 10/3$ .

device along  $y$  direction is limited, a small part of the detecting wave may impinge onto the slope sides of our device, and consequently leads to small scatterings. However, compared with the cases when our ONM structure is removed, one sees that our device can greatly reduce the scattering of the PEC square (see Figs. 2(b)–(e)).

### 3. REALIZATION DESIGN

To realize the necessary ONM, we use metallic plates that satisfy Fabry-Perot resonance conditions [27]. In our design, the thickness of ONMs along its main axis is fixed ( $\sqrt{2}d$ ). We can use metallic plates whose length satisfies  $L = \sqrt{2}d = m\lambda_0$  ( $m = 1, 2, 3, \dots$ ) along the  $+45$  and  $-45$  to realize the ONMs in the regions II & IV and regions I & III, respectively. The basic structure to realize OIC by metallic plates is shown in Fig. 3(a). The metal acts as a perfect electric conductor (PEC) in our design for the microwave frequency range. When the period is much smaller than the wavelength of incident

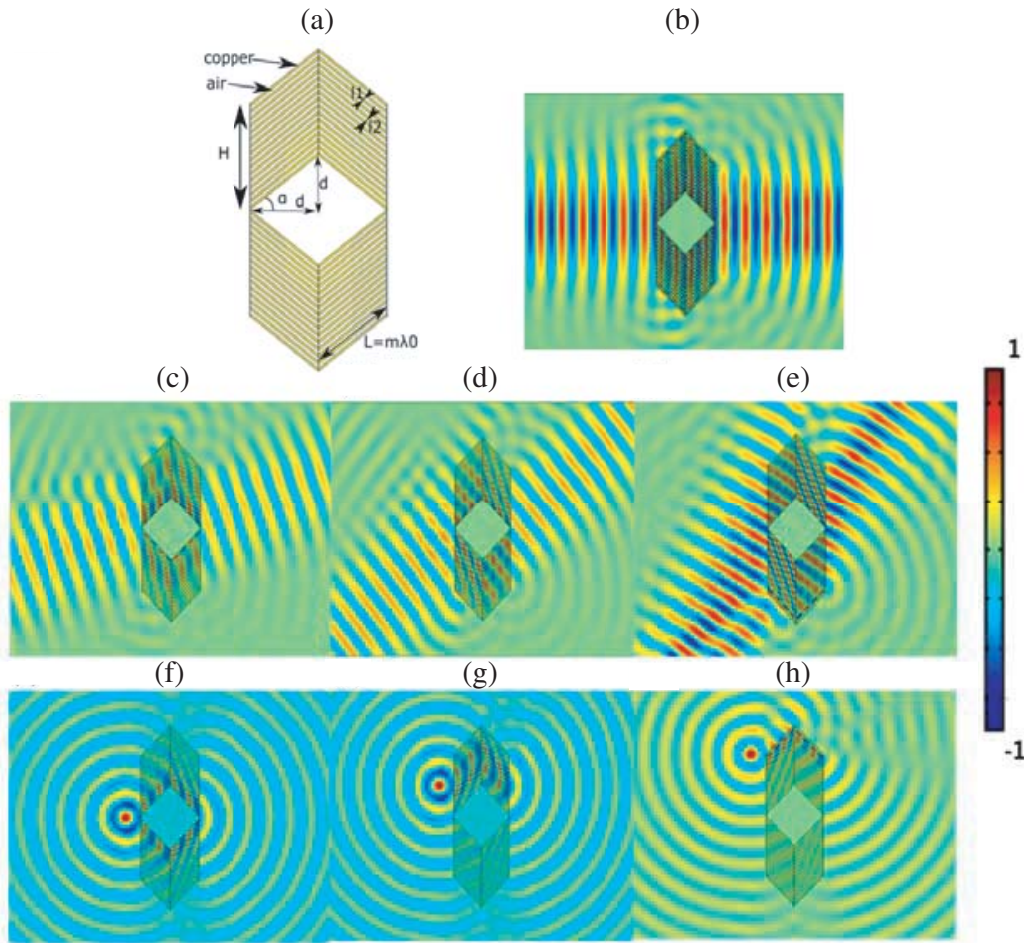


**Figure 3.** (a) The schematic diagram to realize the camouflage device in Fig. 2(a) by metallic plates. The metallic plates (colored yellow) with fixed length  $L = m\lambda_0 = 5.66$  cm ( $\lambda_0 = 2.83$  cm and  $m = 2$  satisfying F-P resonance condition) and thickness  $l_1 = 1.5$  mm. The thickness of each air layer is  $l_2 = 2$  mm. All other regions are air. The geometrical size of the camouflage device here are  $H = 6.65$  cm,  $d = 4$  cm, and  $\alpha = 45$  degree. (b)–(h) are 2D numerical simulations for the snapshots of the normalized magnetic field's  $z$  component distribution. (b)–(e) are cases that the incident detecting waves are Gaussian beams with the same waist radius  $w_0 = 2\lambda_0$  when the incident angles change from 0 degree to 60 degree by a 20 degree step. (f)–(h) are cases that the detecting waves are produced by a magnetic line current source.

electromagnetic wave, the layered structure of PEC and air can be treated as an effective medium with extreme anisotropy satisfying the condition of an ONM [27]. The direction of the metallic plates is the same as the direction of the ONM's main axis. We only use simple uniform copper plates to realize an ONM in the microwave regime and combine these structures to achieve our camouflage device. The performance of the camouflage device realized by metallic plates in Fig. 3(a) is verified by numerical simulations (see Figs. 3(b)–(h)). Our device consists of copper plates and concealed region which are larger than the working wavelength and can be arbitrarily scaled using the same OST designs without new requirements for the ONM.

#### 4. BANDWIDTH

The camouflage device based on the ONMs can still work if the wavelength is detuned from the designed wavelength. Fig. 4(a) shows the normalized scattered power from a PEC square with and without the camouflage device when the wavelength varies. The normalized scattered power is defined as ratio of the surface integration of the scattered Poynting vector on an enclosure space (enclosing the camouflage device) to the incident power of the detecting Gaussian beam. The camouflage device can effectively reduce the scattering of the PEC square for a broadband frequency range. We also plot the electric field distribution when the wavelength is at the designed one and off the designed one in Figs. 4(b) and (c), respectively. When the wavelength is off the designed one, the scattering is mainly due to the reflection. As the wavelength becomes much smaller than the designed one, each copper-air pair in our structure

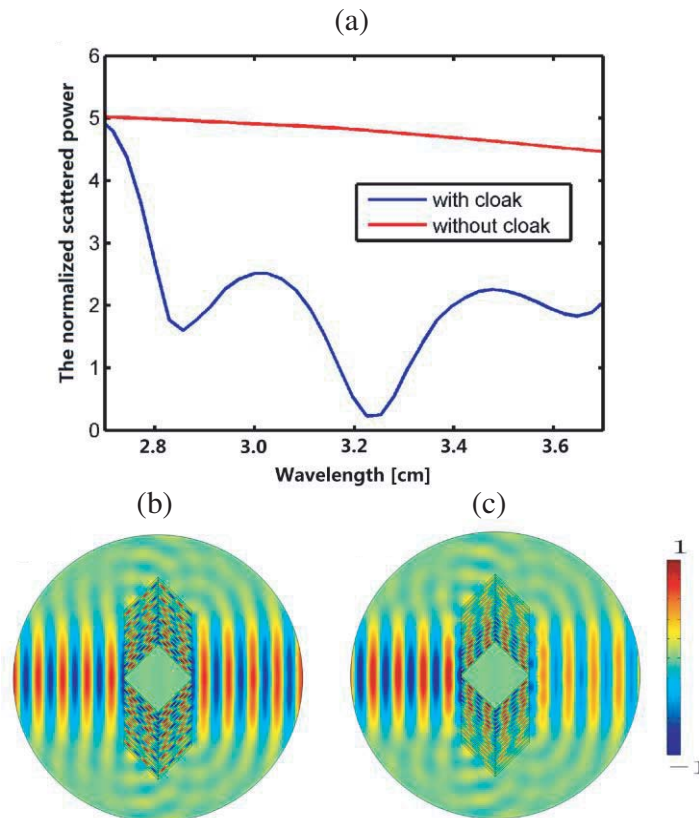


**Figure 4.** (a) The normalized scattered power when the wavelength varies for the cases with our camouflage device (blue) and without the camouflage device (red). The detecting wave is a Gaussian beam with the same size as in Fig. 2 with an incident angle of 0 degree. The geometrical size of the camouflage device is the same as the designed one in Figs. 2(a). (b) and (c) are 2D numerical simulation results for the snapshots of the distributions for the normalized magnetic field's  $z$  component when the wavelength is at and off the designed one, respectively.

cannot be treated as the effective medium for the detecting wave, and consequently the camouflage device will lose its function gradually.

## 5. THE LATERAL DISPLACEMENT (PHASE SHIFT) PROBLEM

Although our camouflage device can keep the magnitude and wave front of incident detecting wave undisturbed, there is lateral displacement (phase shift) of the point source for the viewer on the right side (the source seems closer to the observer on its right side in Figs. 3(f)–(h)). That is the main difference between our camouflage device and perfect invisibility cloaking. The lateral displacement (phase shift) is due to the special feature of ONM: the region filled by ONM is ‘optic-null’. Since electromagnetic field distribution on the input surface is perfectly projected onto the output surface of our ONM device, it seems that the spatial region between the input surface and output surface of the ONM device does not exist, i.e., an “optic-null space”. A restoring layer that can compensate the “optic-null space” produced by ONM has been designed to fix this problem. The restoring layer is designed by a spatial compression coordinate transformation with the help of transformation optics. As shown in Fig. 5(a), a restoring layer with thickness  $t$  is added on the right surface of the camouflage device (with a total length of  $2d$  along  $x$  direction). Since the camouflage device filled by ONM is optic-null space, the whole effective space of the system in Fig. 5(a) (the camouflage device and the

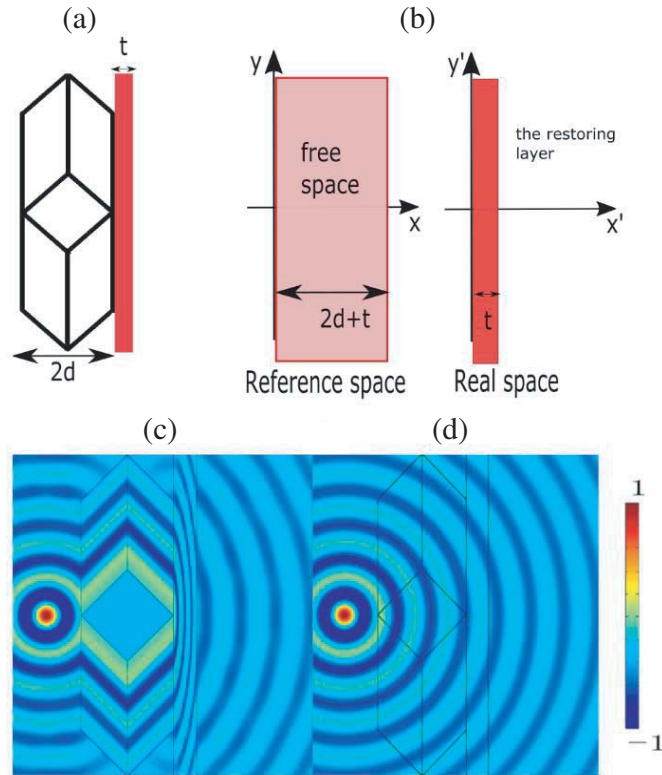


**Figure 5.** (a) Fix the phase shift problem by adding a restoring layer on the right surface of the camouflage device. (b) The coordinate transformation relation in the reference space (Left) and the real space (Right) to design the restoring layer by Transformation Optics. (c) shows the 2D numerical simulation results when the designed restoring layer is added to the camouflage device. The size of the camouflage device is the same as the one in Fig. 2. The thickness of the restoring layer is  $t = 2\lambda_0/3$ . The detecting waves are produced by a magnetic line current source in front of the cloak. (d) shows the comparison situation when we remove the camouflage device, restoring layer and PEC square (just a magnetic line current in free space).

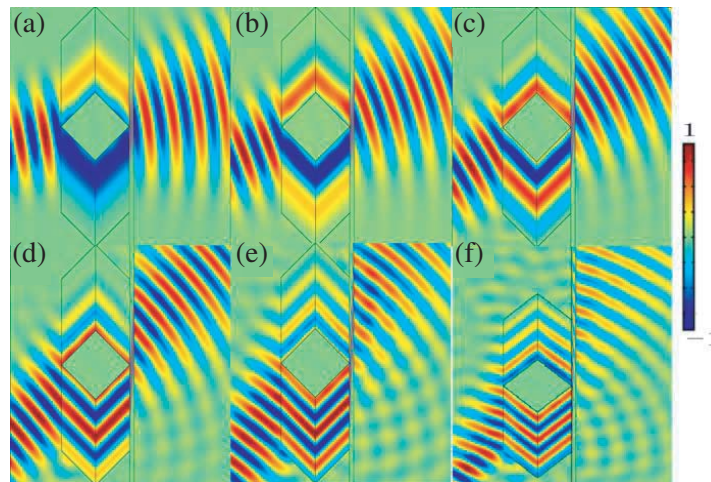


**Figure 6.** 2D numerical simulations when the restoring layer described by Eq. (3) is added on the right surface of the camouflage device for the Gaussian beam detecting case: we plot the snapshots of the normalized magnetic field’s  $z$  component distribution for the TM wave case. (a)–(f) The incident angles of the Gaussian beams are 10, 20, 30, 40, 50 and 60 degrees. Note that we scale the figure in (f) to see a larger computation domain. The sizes of the Gaussian beam and the camouflage device are the same as the case considered for Fig. 2. The thickness of the restoring layer is  $t = \lambda_0/6$ .

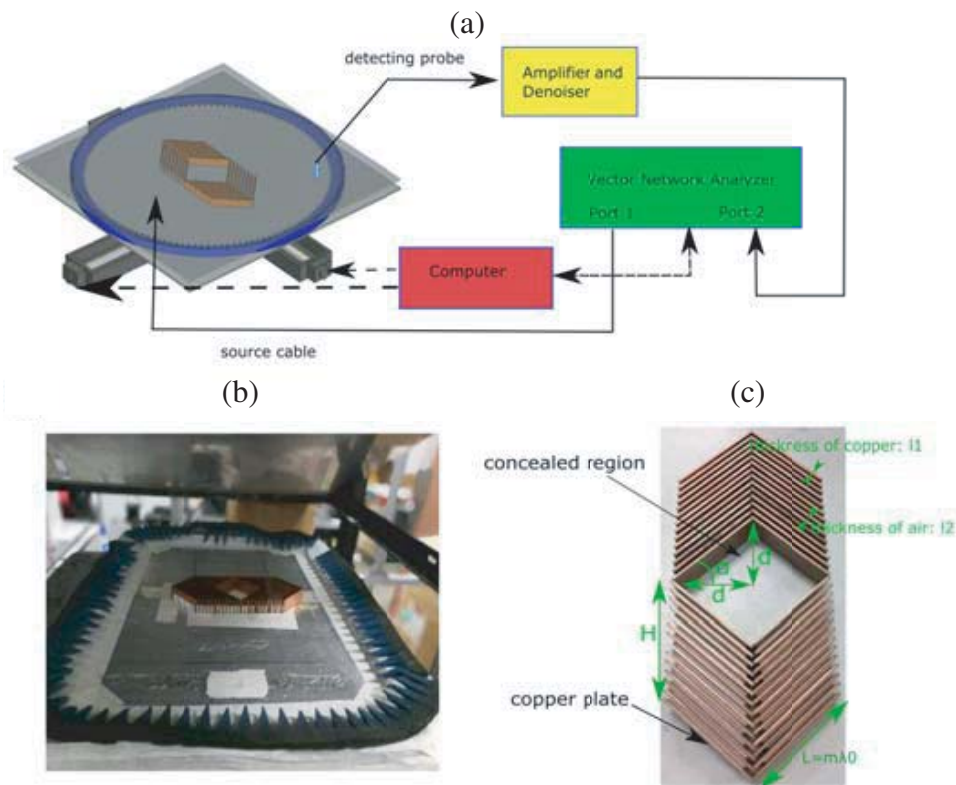


**Figure 7.** (a) and (b) are the sketch map and photograph of the measurement system. (c) The photograph of our OIC by copper plates. The length and thickness of copper plates are  $L = m\lambda_0 = 5.66$  cm ( $\lambda_0 = 2.83$  cm and  $m = 2$ ; satisfying F-P resonance condition) and  $l_1 = 1.5$  mm, respectively. The thickness of each air layer is  $l_2 = 2$  mm. The geometrical size of the cloak here are  $H = 6.65$  cm,  $d = 4$  cm, and  $\alpha = 45$  degree.

restoring layer together) exactly equates to the effective space of the restoring layer. Then we fill some special medium inside the restoring medium to make its effective space equate to a free space region with thickness  $2d + t$  along  $x$  direction. This can be made by a spatial compression transformation of transformation optics (see Fig. 5(b)): a free space with thickness  $2d + t$  along  $x$  direction is compressed into a slab region (the restoring layer) with thickness  $t$  along  $x'$  direction:

$$\begin{cases} x' = \frac{t}{2d+t}x \\ y' = y \\ z' = z \end{cases}. \quad (2)$$

Here we use quantities with and without primes to indicate the quantities in the real and reference spaces, respectively [1–3]. With the help of transformation optics, the required permittivity and permeability of the restoring layer can be given by:

$$\varepsilon' = \mu' = \text{diag} \left( \frac{t}{2d+t}, \frac{2d+t}{t}, \frac{2d+t}{t} \right). \quad (3)$$

If we add such a restoring layer described by Eq. (3) on the right surface of the camouflage device, the lateral displacement problem of the point source can be fixed (see Figs. 5(c) and (d)). Note that there are some small disturbances on the wave front, which is due to the limited size of our cloak.

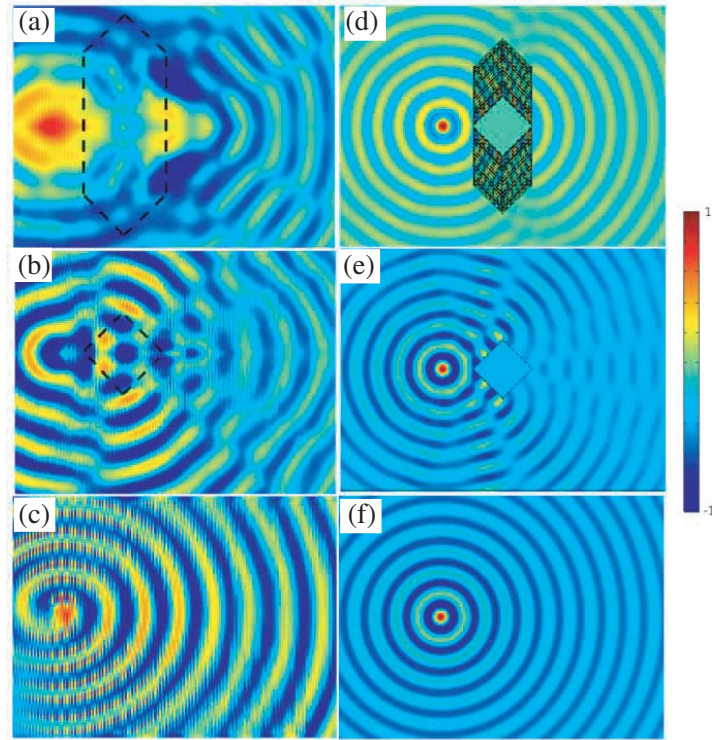


**Figure 8.** (a)–(c) The distribution for the measured normalized magnetic flux density’s  $z$  component in the waveguide system. (d)–(f) 2D numerical simulation results corresponding to the measured (a)–(c), respectively. The designed working wavelength is 2.83 cm. (a) and (d): our designed cloak is around the concealed object (a PEC square) when the detecting line current source is on the left side of the structure. The location of our cloak is indicated by the black dashed line. (b) and (e): only the PEC square is set on the right side of the detecting line current source (the cloak is removed). The location of the PEC square is indicated by the black dashed line. (c) and (f): only a line current source is in free space (both cloak and PEC square are removed).

When the restoring layer is applied (see Fig. 5(c)), the viewer at the right side cannot find any lateral displacement (i.e., the wave on the right side looks like the wave produced by a point source in free space in Fig. 5(d)). In this case, our camouflage device can work as an invisibility cloak.

If the detecting wave is a Gaussian beam as shown in Figs. 2(b)–(e), there is also a lateral displacement for the output beam. This is also due to the ‘optic-null’ feature of the ONM: the electromagnetic field on the input surface of the ONM device is exactly projected to the output surface of the ONM device, and the spatial region filled with ONMs can be considered as of non-existence. The restoring layer given in Eq. (3) can compensate the ‘optic-null space’ produced by ONM and thus the lateral displacement problem for the Gaussian beam detecting case is also fixed (see Fig. 6).

## 6. EXPERIMENTAL MEASUREMENT

We perform experimental characterization in a 2D planar waveguide system (Figs. 7(a) and (b)) with two big aluminum planes to form the 2D planar waveguide. The separation between the upper aluminum plane and the lower aluminum plane is 2 cm. The fabricated cloak (Fig. 7(c)) consists of copper plates, and some foamed plastic materials ( $\epsilon_r = \mu_r = 1$  in the microwave frequency) are used in the bottom to firmly fix the copper plates. Figs. 8(a)–(c) are the measured results when wavelength is the designed one (e.g.,  $\lambda_0 = 2.83$  cm). Figs. 8(d)–(f) give the numerical simulation results corresponding to the measured results in Figs. 8(a)–(c), respectively.

## 7. DISCUSSION AND CONCLUSION

Very recently, two designs have been published by adopting eps-nearly-zero materials and perfect electric conductor to achieve invisibility cloaks [28, 29]. Although their cloaks also require ONM for realization, their designing processes are still based on traditional TO (i.e., involve complex coordinate transformation and tensor calculations). Our design in this study is based on the OST, which is a graphical designing method. OST is a surface-to-surface directional projecting method without any mathematical calculations. The whole designing process of the OST is to choose suitable geometrical shapes of input/output surfaces and the directions of the ONMs between these two surfaces. Our method is much simpler and flexible than TO. For the recent work on an omnidirectional cloak [28], the design is still a spatial stretching-compressing coordinate transformation. Just some regions of the cloak require ONMs and the remaining regions require other materials. The whole camouflage device of our design only requires the same ONMs for realization. Another recent study [29] on invisibility cloak has a similar structure as our camouflage device. However, their cloak still has the phase shift problem, which can be fixed by some restoring layer in our design (see Figs. 5 and 6). Their method is the further coordinate transformation inside the transformation-invariant medium (i.e., ONM), which also needs coordinate transformations and mathematical calculations. We also made some studies on the further coordinate transformation inside the transformation-invariant medium in 2014 [30]. However, the camouflage device in this study is designed by our novel optical design method (i.e., OST) without involving any mathematical calculations. Actually our structures were proposed much earlier than those in the recent work [29] (we have proposed in a straightforward way the same/similar designs much earlier in 2018; see, e.g., our patents filed in early 2018 on the same camouflage device [31] and retro-reflectors [32]).

Note that the camouflage device by perfect ONM (given in Eq. (1)) is independent on the polarization of the detecting waves. However, as metallic plates (satisfy Fabry-Perot resonance conditions) can effectively realize ONM only for the TM polarized beams, the camouflage device by metallic plates in Figs. 3 and 4 can only work for TM polarized beams. In this study, all detecting waves in numerical simulations are the TM waves. All full-wave numerical simulations are made by commercial software COMSOL Multiphysics 5.3 (wave optics package in frequency domain). We choose free triangular meshing with a maximum element size of one over ten working wavelengths.

In conclusion, the function of the metallic plates array designed here is like many perfect endoscopes, which can guide the detecting wave around the concealed objects and redirect it back to the original direction. Designing a camouflage device using the OST graphical method is simpler and more

convenient than transformation optics. The proposed camouflage device can work for both wide-angle-incident plane waves and line current source, which can be realized by one homogeneous ONM. A simple array of metallic plates where the length of each plate satisfies the F-P resonance condition can serve as an effective ONM. Our camouflage device can effectively reduce the scattering of the PEC square in a broad frequency band. The proposed camouflage device is realized by just one material with robust performance verified by numerical simulations. The proposed method provides a new way to design camouflage device, which can potentially be extended to 3D case and applied in different wavelength regimes.

## ACKNOWLEDGMENT

This work is partially supported by the National Natural Science Foundation of China (Nos. 61971300, 11604292, 61905208, 11674239, 91833303, 11621101, 91233208 and 60990322), the Scientific and Technological Innovation Programs (STIP) of Higher Education Institutions in Shanxi (Nos. 2019L0159 and 2019L0146), the Postdoctoral Science Foundation of China (Nos. 2017T100430 and 2018M632455), the National Key Research and Development Program of China (No. 2017YFA0205700), the Program of Zhejiang Leading Team of Science and Technology Innovation, and AOARD.

## REFERENCES

1. Pendry, J. B., D. Schurig, and D. R. Smith, "Controlling electromagnetic fields," *Science*, Vol. 312, 1780, 2006.
2. Chen, H., C. T. Chan, and P. Sheng, "Transformation optics and metamaterials," *Nat. Mater.*, Vol. 9, 387, 2010.
3. Sun, F., B. Zheng, H. Chen, W. Jiang, S. Guo, Y. Liu, Y. Ma, and S. He, "Transformation optics: From classic theory and applications to its new branches," *Laser Photonics Rev.*, Vol. 11, 1700034, 2017.
4. Schurig, D., J. J. Mock, B. J. Justice, S. A. Cummer, J. B. Pendry, A. F. Starr, and D. R. Smith, "Metamaterial electromagnetic cloak at microwave frequencies," *Science*, Vol. 314, 977, 2006.
5. Cai, W., U. K. Chettiar, A. V. Kildishev, and V. M. Shalaev, "Optical cloaking with metamaterials," *Nat. Photonics*, Vol. 1, 224, 2007.
6. Landy, N. and D. R. Smith, "A full-parameter unidirectional metamaterial cloak for microwaves," *Nat. Mater.*, Vol. 12, 25, 2013.
7. Shen, L., B. Zheng, Z. Liu, Z. Wang, S. Lin, S. Dehdashti, E. Li, and H. Chen, "Large-scale far-infrared invisibility cloak hiding object from thermal detection," *Adv. Opt. Mater.*, Vol. 3, 1738, 2015.
8. Chen, H., B. Zheng, L. Shen, H. Wang, X. Zhang, N. I. Zheludev, and B. Zhang, "Ray-optics cloaking devices for large objects in incoherent natural light," *Nat. Commun.*, Vol. 4, 2652, 2013.
9. Zheng, B., R. Zhu, L. Jing, Y. Yang, L. Shen, H. Wang, Z. Wang, X. Zhang, X. Liu, E. Li, and H. Chen, "3D visible-light invisibility cloak," *Adv. Sci.*, Vol. 5, 1800056, 2018.
10. Ma, Y., Y. Liu, L. Lan, T. Wu, W. Jiang, C. K. Ong, and S. He, "First experimental demonstration of an isotropic electromagnetic cloak with strict conformal mapping," *Sci. Rep.*, Vol. 3, 2182, 2013.
11. Ma, Y., L. Lan, W. Jiang, F. Sun, and S. He, "A transient thermal cloak experimentally realized through a rescaled diffusion equation with anisotropic thermal diffusivity," *NPG Asia Mater.*, Vol. 5, e73, 2013.
12. Zhang, S., C. Xia, and N. Fang, "Broadband acoustic cloak for ultrasound waves," *Phys. Rev. Lett.*, Vol. 106, 024301, 2011.
13. Gömöry, F., M. Solovyov, J. Šouc, C. Navau, J. Prat-Camps, and A. Sanchez, "Experimental realization of a magnetic cloak," *Science*, Vol. 335, 1466, 2012.
14. Zhu, J., W. Jiang, Y. Liu, G. Yin, J. Yuan, S. He, and Y. Ma, "Three-dimensional magnetic cloak working from dc to 250 kHz," *Nat. Commun.*, Vol. 6, 8931, 2015.

15. Li, J. and J. B. Pendry, "Hiding under the carpet: A new strategy for cloaking," *Phys. Rev. Lett.*, Vol. 101, 203901, 2008.
16. Liu, R., C. Ji, J. J. Mock, J. Y. Chin, T. J. Cui, and D. R. Smith, "Broadband ground-plane cloak," *Science*, Vol. 323, 366, 2009.
17. Chen, X., Y. Luo, J. Zhang, K. Jiang, J. B. Pendry, and S. Zhang, "Macroscopic invisibility cloaking of visible light," *Nat. Commun.*, Vol. 2, 176, 2011.
18. Sun, F. and S. He, "Optical surface transformation: Changing the optical surface by homogeneous optic-null medium at will," *Sci. Rep.*, Vol. 5, 16032, 2015.
19. Sun, F. and S. He, "Surface transformation with homogenous optic-null medium," *Progress In Electromagnetics Research*, Vol. 151, 169–173, 2015.
20. Guo, S., F. Sun, and S. He, "Optical surface transformation for reshaping the field intensity distribution," *J. Opt. Soc. Am. B*, Vol. 33, 1847, 2016.
21. Sun, F., X. Ge, and S. He, "Creating a zero-order resonator using an optical surface transformation," *Sci. Rep.*, Vol. 6, 21333, 2016.
22. Sun, F. and S. He, "Overlapping illusions by transformation optics without any negative refraction material," *Sci. Rep.*, Vol. 6, 19130, 2016.
23. Sun, F. and S. He, "Waveguide bends by optical surface transformations and optic-null media," *J. Opt. Soc. Am. B*, Vol. 35, 944, 2018.
24. Sun, F. and S. He, "Optic-null space medium for cover-up cloaking without any negative refraction index materials," *Sci. Rep.*, Vol. 6, 29280, 2016.
25. Sun, F. and S. He, "Subwavelength focusing by optical surface transformation," *Opt. Commun.*, Vol. 427, 139, 2018.
26. Rahm, M., S. A. Cummer, D. Schurig, J. B. Pendry, and D. R. Smith, "Optical design of reflectionless complex media by finite embedded coordinate transformations," *Phys. Rev. Lett.*, Vol. 100, 063903, 2008.
27. Sadeghi, M. M., S. Li, L. Xu, B. Hou, and H. Chen, "Transformation optics with Fabry-Pérot resonances," *Sci. Rep.*, Vol. 5, 8680, 2015.
28. Zheng, B., Y. Yang, Z. Shao, Q. Yan, N. H. Shen, L. Shen, H. Wang, E. Li, C. M. Soukoulis, and H. Chen, "Experimental realization of an extreme-parameter omnidirectional cloak," *Research*, Vol. 2019, 8282641, 2019.
29. Zhang, Y., Y. Luo, J. B. Pendry, and B. Zhang, "Transformation-invariant metamaterials," *Phys. Rev. Lett.*, Vol. 123, 067701, 2019.
30. Sun, F. and S. He, "Extending the scanning angle of a phased array antenna by using a null-space medium," *Sci. Rep.*, Vol. 4, 6832, 2014.
31. He, S. and F. Sun, "A new invisibility structure in upper air," Chinese Patent; public number: CN108808259A (publication date: November 13, 2018), <https://www.tianyancha.com/patent/acee8373a11f5d53301f05da263799fd>.
32. He, S., F. Sun, and Y. Liu, "A novel optical retro-reflector and retro-reflection array," Chinese Patent; public number: CN108415109A (publication date: August 17, 2018), <https://www.tianyancha.com/patent/7584015d358172d59ae7dd902a7892f9>.